Carbohydrate Polymers 87 (2012) 353–360

Contents lists available at ScienceDirect

Carbohydrate Polymers

journal homepage: www.elsevier.com/locate/carbpol

Chalcone embedded polyurethanes as a biomaterial: Synthesis, characterization and antibacterial adhesion

Ponnurengam Malliappan Sivakumar[a,b,*], Stefania Cometa[b], Michele Alderighi[b], Veluchamy Prabhawathi[a], Mukesh Doble[a], Federica Chiellini[b]

[a] Department of Biotechnology, Indian Institute of Technology Madras, Chennai 600036, India
[b] Laboratory of Bioactive Polymeric Materials for Biomedical and Environmental Applications (BIOlab), UdR INSTM, Department of Chemistry & Industrial Chemistry, University of Pisa, Pisa, Italy

ARTICLE INFO

Article history:
Received 4 May 2011
Received in revised form 28 July 2011
Accepted 28 July 2011
Available online 5 August 2011

Keywords:
Polyurethane
Chalcone
Bacterial adhesion
SEM EDAX
AFM

ABSTRACT

An antibacterial dimethylamino-chalcone embedded multiblock copolymer (PCL–PEG) was synthesized and characterized using FT-IR, ^{1}H NMR, SEM and SEC and the compound was characterized using FT-IR, ^{1}H NMR, and ^{13}C NMR. A 10% copolymer composite was prepared and casted as film to be used as a biomaterial and the copolymer films without the compound acted as control. TGA, DSC, AFM, SEM and EDAX analysis were performed for the above samples. Surface roughness (R_a) of the copolymer composite film was less when compared to the copolymer film which indicated the proper distribution of chalcone in the composite film. copolymer composite film was hydrophilic compared to copolymer film. Antibacterial adhesion studies were performed for copolymer composite polymer film and evaluated using CFU measurement and SEM analysis. Copolymer composite film shows promising antibacterial adhesion compared to the copolymer film. Hence the copolymer composite film can be used as a new biomaterial endowed with antibacterial properties.

1. Introduction

Formation of biofilm and colonization of bacteria on medical implants leads to infection. The usage of the medical implants has led to increased incidence of nosocomial infections accounting to around two million cases in United States alone (Nablo, Prichard, Butler, Klitzman, & Schoenfisch, 2005). Medical implants, including urinary catheters, central venous catheters and endotracheal tubes, play significant contribution towards implant associated infections (Klevens et al., 2002). *Staphylococcus epidermidis* is the major organism related to device-oriented nosocomial infections (Rupp & Archer, 1994). Bacteria can attach either directly to the polymeric material or to the proteins adsorbed on the polymeric surface, colonizing (biofilm formation) and then spreading and producing the systemic toxicity. Biofilm protects bacteria from immune system and antibacterial therapies (Vuong & Otto, 2002).

Methicillin resistant *S. aureus* (MRSA) and fluoroquinolone resistant *Escherichia coli* were found at increased frequencies in hospital acquired infections in United States ICUs. Coagulase positive *S. aureus*, coagulase-negative *S. aureus*, *E. coli* and *Pseudomonas aeruginosa* are also found with device related infections (Pierce, 2005; Schulin & Voss, 2001).

Polyurethanes (PU) are widely used in the preparation of medical devices due to their biocompatibility, ability to promote the cell adhesion (Cometa, Bartolozzi, et al., 2010; Cometa, Chiellini, et al., 2010) and to act against bacterial adhesion when compared to other polymers (Flemming, Capelli, Cooper, & Proctor, 2000; Khandwekar, Patil, Shouche, & Doble, 2009).

One of the strategies to prevent the bacterial attachment and biofilm formation is to kill the bacterial cells when they come in contact with the polymeric surfaces (Sivakumar, Iyer, Natesan, & Doble, 2010). Hence previous studies mixed bactericidal and fungicidal agents with PU, PMMA, PET and other polymers to reduce the bacterial infections (Grapski & Cooper, 2001; Nava-Ortiz et al., 2010). Other strategies include use of molecules which can interfere with quorum sensing of the bacteria, dissolve biofilms (Francolini et al., 2010), or change the surface energy of the polymer.

Chalcones are a class of compounds available, both in naturally and synthetic form. They exert a wide variety of biological functions including anti-tubercular (Sivakumar, Seenivasan, Kumar, & Doble, 2007), antifungal (Sivakumar, Kumar, & Doble, 2009) and broad spectral antibacterial activities (Sivakumar, Priya, & Doble, 2009; Selvakumar et al., 2007). They exert their antibacterial activity by the disruption of the cell membrane (Nielsen, Larsen, Boesen, Schønning, & Kromann, 2005). Chalcones are also used in medical devices either as coating or as a composite with polymer. Due to

* Corresponding author at: Department of Biotechnology, Indian Institute of Technology Madras, Chennai 600036, India. Tel.: +91 44 2257 4107; fax: +91 44 2257 4102.
E-mail address: sivamedchem@yahoo.co.in (P.M. Sivakumar).

0144-8617/$ – see front matter © 2011 Elsevier Ltd. All rights reserved.
doi:10.1016/j.carbpol.2011.07.061

their slimicidal activity, chalcones also prevent the colonization of bacteria (Sivakumar, Priya, et al., 2009).

In the present study, a new composite based on multiblock copolymer (PCL–PEG) and chalcone was synthesized, characterized and its antibacterial properties were assessed. There is a need for design and synthesis of newer polymer based biomaterial which can prevent the adhesion and colonization of bacteria.

2. Materials and methods

2.1. General aspects

The macrodiols, *i.e.* PEGdiol3400 and PCLdiol2000, HMDI (Hexamethylene diisocynate), tin(II) 2-ethylhexanoate were purchased from Sigma–Aldrich, Italy. Solvents used for the study were purchased from J.T. Baker, Italy. The strains used in this study namely, *S. aureus* NCIM 5021 and *E. coli* NCIM 2931 were purchased from National Chemical Laboratory (NCL), Pune, India and were maintained in nutrient agar plates. All broth and agar reported here were purchased from Himedia, India.

2.2. Synthesis of dimethylamino chalcone

Chalcone was synthesized by the method reported by Lin, Rivett, and Wilshire (1977) using dimethylamino-benzaldehyde and acetophenone and characterized using Fourier Transform Infrared (FT-IR) Spectroscopy, ^{1}H NMR and ^{13}C NMR.

2.3. Polymerization

Calculated amount of PCLdiol2000 and PEGdiol3400 were dried under nitrogen atmosphere overnight. HMDI was distilled before use in the reaction. PCLdiol2000 and PEGdiol3400 were mixed together in the ratio of 75:25 in a polymeric tube under nitrogen atmosphere. Stoichiometric amount of HMDI was added to the above mixture and was followed by a few drops of tin(II) 2-ethylhexanoate. The polymeric tube was sealed and was placed in an oil bath and heated to 60 °C for 2 h and then to 70 °C for 1 h under vigorous stirring. The resultant polymer synthesized was solubilized in chloroform and then precipitated with petroleum ether and diethyl ether in order to remove the unreacted monomers. The precipitated polymer was dried under vacuum for 48 h.

2.4. Bulk characterization of copolymer

The bulk characterization of the synthesized copolymer was performed using ^{1}H NMR (Varian Gemini 200), FT-IR (Jasco FT/IR-410) and size exclusion chromatography (Jasco PU-1580). Size Exclusion Chromatography (SEC) analysis was performed using High-Performance Liquid Chromatograph (HPLC) connected to a Jasco 830-RI and PerkinElmer LC-75 spectrophotometric (λ = 260 nm) detectors, equipped with two mixed-D PLgel columns (300 mm × 7.5 mm). Chloroform was used as eluting solvent and the calibration curve was plotted using mono-dispersed polystyrene standards.

2.5. Film preparation

One gram of the synthesized copolymer was solubilized in 15 ml of chloroform. 100 mg of chalcone (10% weight to the polymer weight) were added to the polymeric solution and mixed thoroughly. Then the solution was cast in a Petri dish and the solvent was allowed to evaporate for 3 days. The film that was formed was kept under vacuum for 1 day to remove the solvent. 1 cm × 1 cm pieces were cut from the film (copolymer composite film) and used for further studies. Films were also cast without chalcone (copolymer film) and were used as control in all the studies.

2.6. Thermal characterization of copolymer

The thermal degradation pattern of the synthesized copolymer (before the copolymer was casted in to a film), copolymer film, chalcone (the synthesized compound) and copolymer composite film were evaluated using a Thermo gravimetric analyser (TGA) (TGAQ500 MFC system). The samples were heated at a rate of 10 °C per minute from 30 °C to 600 °C in the presence of nitrogen.

Differential Scanning Calorimetry (DSC) was also used to study the thermal characteristics of the copolymer, copolymer film, chalcone and copolymer composite film using Mettler TA4000 instrument. The sample was first heated from 30 °C to 150 °C at a heating rate of 10 °C/min and then cooled from 150 °C to −100 °C at a cooling rate of 10 °C/min, followed by 4 min at this temperature. The second heating scan was run from −100 °C to 120 °C at a heating rate of 10 °C/min. Samples of 6–7 mg were taken in a 40 μl aluminum pan while an empty pan was used as reference. Measurements were carried out under nitrogen atmosphere at a flow rate of 80 ml/min.

2.7. Surface characterization of the polymeric films

2.7.1. Fourier Transform Infrared (FT-IR) Spectroscopy

Jasco FT/IR-410 instrument was used to record the FT-IR spectrum of the copolymer film, chalcone and copolymer composite film in the range of 400–4000 cm^{-1}.

2.7.2. Atomic force microscopy (AFM)

AFM measurements were performed by a multimode instrument connected to Nanoscope IV controller and equipped with E piezoelectric scanner (Veeco Metrology). Contact mode was used to determine the surface roughness of the films.

2.7.3. Static contact angle and surface energy measurements

Surface energy and static contact angle (SCA) of the films were measured with HPLC-grade water and n-hexadecane using the sessile drop method at 25 ± 0.1 °C with a DSA 10 drop shape analysis system (Kruss, Hamburg, Germany).

One wt.% copolymer solution in chloroform was filtered on a 0.45 mm nylon filter, dropped on the surface of a microscope glass plate and spin coated at 6200 rpm for 60 s. The film was kept in a dry atmosphere and was used for contact angle measurements.

2.7.4. Scanning Electron Microscopy (SEM)

The surface morphology of the copolymer, copolymer film and polymer composite film were determined using a JEOL LSM5600LV (Tokyo, Japan) scanning electron microscope. The samples were gold sputtered under high vacuum before the analysis. EDAX studies were also performed for copolymer and copolymer composite films to determine the composition of the surfaces.

2.8. Bacterial adhesion

Bacterial adhesion experiments were carried out as previously reported with slight modifications (Zhao et al., 2007). A single colony from Petri plate was inoculated into a 100 ml conical flask containing 20 ml of tryptic soy broth (TSB). It was cultured for 16 h in a shaker (Orbitech, India) at 180 rpm and 37 °C until it reached mid-exponential phase. The culture was centrifuged at 8000 rpm and 4 °C for 10 min. The pellets were resuspended in 0.9% saline and adjusted to an optical density (O.D.) of 0.1 at 660 nm (which is approximately 1 × 10^{7} cells/ml). The copolymer and copolymer

composite films were immersed in 20 ml of the above bacterial suspension and were incubated under static conditions at 37 °C for 2 h. At the completion of this time period, the samples were transferred into fresh tryptic soy broth and incubated for 24 h at 37 °C and 120 rpm. Then they were removed using sterile forceps and washed gently twice in sterile water to remove non-adhered bacteria. Adhered bacteria were then removed from the polymer surface by water-bath ultrasonication (total of 4 min with 1 min intervals) and counts of viable cells were determined in tryptic soy agar (TSA). All the experiments were repeated thrice.

2.8.1. SEM analysis of bacterial adhesion

The surface of the copolymer film and copolymer composite film (with chalcone) after the adhesion of bacteria were observed under a SEM (Scanning Electron Microscope). The above mentioned films after the bacterial adhesion were washed with distilled water and then fixed with 3% glutaraldehyde (in 0.1% phosphate buffer at pH 7.2) for an hour and then washed twice with phosphate buffer and once using distilled water and dehydrated using various alcohol gradients (20, 50, 70 and 90%) for 10 min and then dried overnight in a dessicator. The films were gold coated at 30 mA for 1 min and viewed under SEM (JEOL JSM 5600 LSV model) at a magnification of 3200×.

2.8.2. Assessment of cell viability and mechanism of action of chalcone

The presence of live and dead microorganisms on the copolymer and copolymer composite films after the bacterial adhesion experiments were determined using Live/Dead® BacLight™ Bacterial Viability Kit (Invitrogen, Germany). The kit consists of two of the dyes namely, SYTO9 and propidium iodide (PI). The PI stains in red only the dead cells, by penetrating into the damaged membrane of the cells. Hence, live cells fluoresce green and dead cells fluoresce red (Boulos, Prévost, Barbeau, Coallier, & Desjardins, 1999). The films after bacterial adhesion were washed with water and placed on a glass slide, stained with the dye, and incubated for 10–15 min in the dark. Then it was covered with coverslip and the images were captured using a Confocal Laser Scanning Microscope (CLSM) (LSM 710 Carl zeiss, Micro Imaging GMBH, Germany). Thickness of the biofilm formed on the surface was also measured using the same instrument. Zen 2009 software was used for data analysis. All images were obtained through a plan-ApoChromate 40×/0.0 Korrm75 objective utilizing 594 (HeNe 594 nm) and 488 (Argon 488) lasers, ch1-493-551 and ch2-598-712 filters and MBS–MBS 488/594 Beam splitter.

3. Results and discussion

3.1. Chalcone synthesis and characterization

The dimethylamino-chalcone was synthesized and characterized using FT-IR, ^{1}H and ^{13}C NMR spectroscopy. Characteristic FT-IR peak is observed at 1648 cm^{-1} which is responsible for α, β-unsaturated carbonyl system present in chalcone. The NMR spectral data for it is given below:

^{1}H NMR ($CDCl_3$, 200 MHz): δ 3.10 (s, 6H), δ 6.77 (d, 2H, J = 8.8 Hz), δ 7.33–7.65 (m, 6H), δ 7.88 (d, 1H, J = 15.4 Hz), δ 8.08 (d, 2H, J = 6.8 Hz). ^{13}C NMR ($CDCl_3$, 50 MHz): δ 190.71, 152.04, 145.87, 139.08, 132.15, 130.43, 128.45, 128.32, 122.63, 116.91, 111.82, 42.00. The structure of the chalcone synthesized and used in the studies is given below:

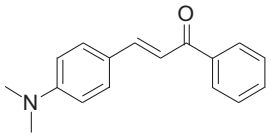

Structure of dimethylamino-chalcone

3.2. Copolymer characterization

The spectral data of the synthesized PCL–PEG multiblock copolymer is given below.

3.2.1. FT-IR

Broad peak at 3450 cm^{-1} (terminal OH), 2944 cm^{-1} and 2867 cm^{-1} (CH_2 aliphatic), 1725 cm^{-1} (C=O ester), 1638 cm^{-1} (C=O amide I), 1527 cm^{-1} (C=O amide II), 1243 cm^{-1} (C–O–C stretching vibrations of repeated –COO– units of PCL back bone), and 1106 cm^{-1} (C–O–C stretching vibrations of repeated O–CH_2–CH_2– units of PEG back bone) observed confirm the presence of different functional groups in the copolymer. These peaks match with the literature reports (Liu, Gong, et al., 2008).

3.2.2. ^{1}H NMR

Characteristic peaks are observed at δ 1.4, 1.7, 2.3 and 4.0 ppm which can be attributed to methylene protons, –$(CH_2)_3$–, –$OCCH_2$– and –CH_2OOC– respectively which are present in the PCL units. The peak at δ 3.6 is responsible for methylene protons in –CH_2CH_2O– of polyethylene glycol repeating units in the block copolymer. Peaks are observed at δ 3.8 and 4.3 which are responsible for the –O–CH_2–CH_2– end in the PEG unit linked with PCL. The ^{1}H NMR peaks at δ 4.0 ppm (–$COCH_2CH_2CH_2CH_2CH_2O$–) and δ 3.6 ppm (–CH_2CH_2O–) can be used to find the ratio of PCL:PEG. Previous researchers have also observed similar results for PCL–PEG–PCL triblock copolymer (Liu, Gong, et al., 2008).

3.2.3. SEC analysis

SEC analysis was performed on the PCL–PEG copolymer. The copolymer Mn resulted equal to 20,500, while the polydispersity index (Mw/Mn) was equal to 3.6, suggesting that, as expected in a polycondensation process, a fairly broad molecular weight distribution were observed.

3.2.4. Thermal characterization of polymer

3.2.4.1. TG analysis. PCLdiol2000 and PEGdiol3400 give a single degradation pattern but the copolymer gives two thermal degradation patterns corresponding to the degradation of the two macro-monomers. Thermal degradation pattern of the copolymer was initiated due to the PCLdiol2000 and it is followed by the degradation of PEGdiol3400. The percentage residue at 600 °C was found to be higher in the case of copolymer when compared to that with PCLdiol2000 or PEGdiol3400.

Fig. 1 shows a comparative thermal decomposition pattern for PCLdiol2000, PEGdiol3400 and block copolymer. The thermogram for the copolymer lies between the thermograms of both monomers. Fig. 2 shows a similar thermogram for chalcone, copolymer film and copolymer composite film from 30 °C to 600 °C. Sharp weight reduction is observed between 250 °C and 350 °C. The thermogram for the composite film lies closely below that of the copolymer film.

The onset temperature (where 2% of the polymer is decomposed) (T_{onset}) and the decomposition temperature (where the maximum amount of decomposition of polymer is achieved) (T_d) are evaluated from TGA for all these materials and listed in Table 1.

Table 1
Onset and decomposition temperatures of monomers, copolymer, copolymer film, chalcone and copolymer composite film.

Component	Onset temperature, T_{onset}	Decomposition temperature			Percentage residue at 600 °C
		T_{d1}	T_{d2}	T_{d3}	
PCLdiol2000	238.35 °C	406.37 °C	–	–	0.60
PEGdiol3400	327.40 °C	397.93 °C	–	–	0.85
PCL–PEG block copolymer	290.63 °C	323.94 °C	404.49 °C	–	2.32
PCL–PEG block copolymer film	305.48 °C	339.35 °C	404.69 °C	–	2.26
Chalcone	185.79 °C	285.31 °C	–	–	0.39
Copolymeric composite film	242.35 °C	265.25 °C	327.31 °C	400.34 °C	2.61

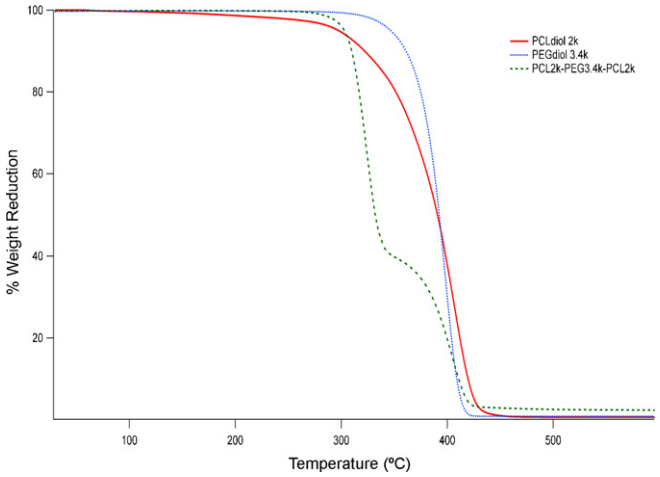

Fig. 1. TGA thermograms of PCLdiol, PEGdiol and copolymer.

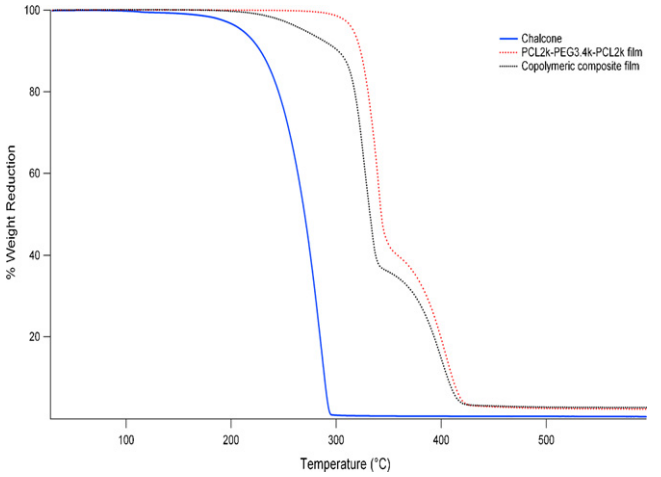

Fig. 2. TGA thermograms of copolymer film, chalcone and copolymer composite film.

Chalcone showed a single degradation pattern which also suggests its purity. As before, copolymer film showed two degradation patterns responsible for PCLdiol2000 and PEGdiol3400. Copolymer composite film showed three thermal degradation patterns corresponding to chalcone, PCLdiol2000 and PEG3400. From the degradation patterns the ratio of the chalcone in the composite was estimated to be 9.58% which is almost equivalent to the amount added during preparation (10%). This suggests that the copolymer composite film is uniformly distributed with chalcone. Figure S1 (supplementary material) shows the percentage of components present in copolymer composite film.

3.2.4.2. DSC analysis. DSC analysis of the various films was performed as mentioned before. Melting, crystallization and glass transition temperatures of first cooling and second heating were calculated and listed in Table 2. The glass transition temperature, melting point and crystallization peaks for PCL and PEG components are in agreement with data reported by the literature (Cometa, Bartolozzi, et al., 2010; Zhou, Deng, & Yang, 2003).

Copolymer and films yield two crystallization peaks during first cooling. The first crystallization peak is due to PEGdiol3350 and the second are due to PCLdiol2000. Copolymer and copolymer films display similar crystallization peaks but copolymer composite film shows crystallization peaks at lower temperature values when compared to other two. This earlier crystallization peaks are due to the incorporation of chalcone and changes in crystalline behaviour of the composite. Organic compound tends to reduce crystallization temperatures.

Copolymer and films during second heating yield two melting points (T_m) and one inflection point and the later is defined as the glass transition temperature (T_g). Copolymer composite film showed the lower melting temperature when compared to copolymer film, due to the presence of chalcone which melts initially and initiates the melting of the monomers.

Fig. 3 shows the DSC spectrum for second heating of copolymer, copolymer film and copolymer composite film. Though there are no extra melting, glass transitions or crystallization peaks, there is a shift in the melting and crystallization peaks which indicate the incorporation of chalcone in the copolymer composite film.

3.3. Surface characterization

Fig. 4 shows the SEM micrographs of copolymer, copolymer film and copolymer composite film. Polymer exhibits an amorphous nature while the cast films show uniform surfaces with indentation. Table 3 shows the weight and atomic percentages of carbon, oxygen and nitrogen contents in copolymer film and copolymer composite

Table 2
DSC analysis of copolymer, copolymer film and copolymer composite film.

Process	Polymer	T_m 1 (°C)	ΔH_f 1 (J/g)	T_m 2 (°C)	ΔH_f 2 (J/g)	T_g (°C)	ΔH_f 3 (J/g k)
Ist cooling	Copolymer	20.61	33.96	27.61	70.80	–	–
	Copolymer film	21.44	38.81	28.27	64.17	–	–
	Copolymer composite film	14.44	27.45	21.77	64.26	−46.53	−0.202
IInd heating	Copolymer	48.10	−62.24	52.43	−45.56	−57.35	0.192
	Copolymer film	48.26	−69.22	52.59	−39.90	−57.52	0.283
	Copolymer composite film	44.09	−45.89	50.42	−43.38	−44.36	0.342

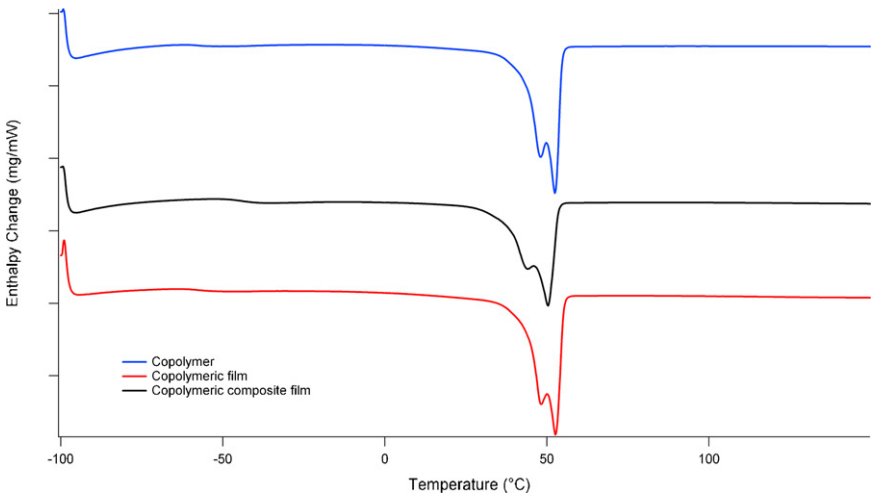

Fig. 3. DSC traces relevant to the second heating of copolymer, copolymer film and copolymer composite film.

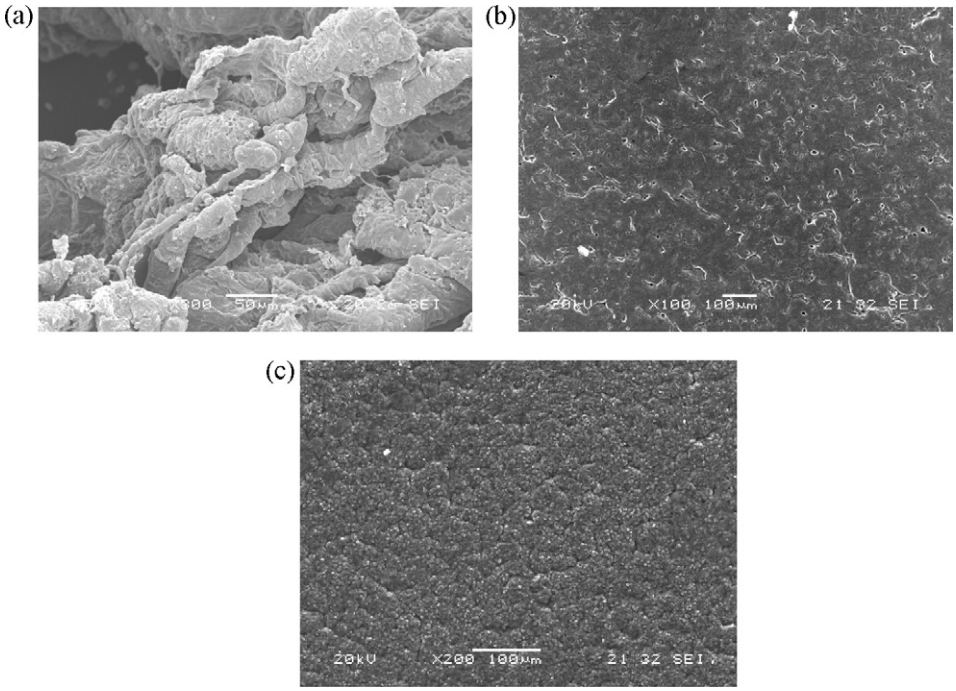

Fig. 4. SEM micrographs of (a) copolymer, (b) copolymer film and (c) copolymer composite film.

film. The copolymer composite film shows increased weight and atomic percentages of nitrogen and carbon, which indicates the incorporation of chalcone into the copolymer cast film.

AFM measurement was performed to analyze the surface roughness and morphology of the copolymer film and copolymer composite film (Fig. 5). The surface roughness of the copolymer composite film (168.33 ± 7.17 nm) was lower than the copolymer film (276.33 ± 20.36 nm). This is due to the uniform distribution of chalcone in the polymer leading to the smoothening of the surface.

Contact angles of the film were measured using water and n-hexadecane. With water, the contact angles of copolymer film and copolymer composite film were 56.4 ± 3.4 and 65.7 ± 7.6 respectively. Being chalcone hydrophobic it increased the water contact angle of the polymer composite film. Rough surface will lead to increase in contact angle of hydrophobic surfaces and reduce the contact angle of hydrophilic surfaces (Liu, Wu, Wei, Cai, & Wei, 2008). With n-hexadecane, the contact angles of copolymer film and copolymer composite film were of 16.2 ± 1.7 and 15.0 ± 1.2,

Table 3
Weight and atomic percentages of various elements in copolymer film and copolymer composite film (based on EDAX).

Element	Copolymer film		Copolymer composite film	
	Weight percentage	Atomic percentage	Weight percentage	Atomic percentage
Carbon	60.77	68.41	72.12	76.57
Oxygen	34.62	29.26	17.15	13.67
Nitrogen	2.12	2.05	10.72	9.76

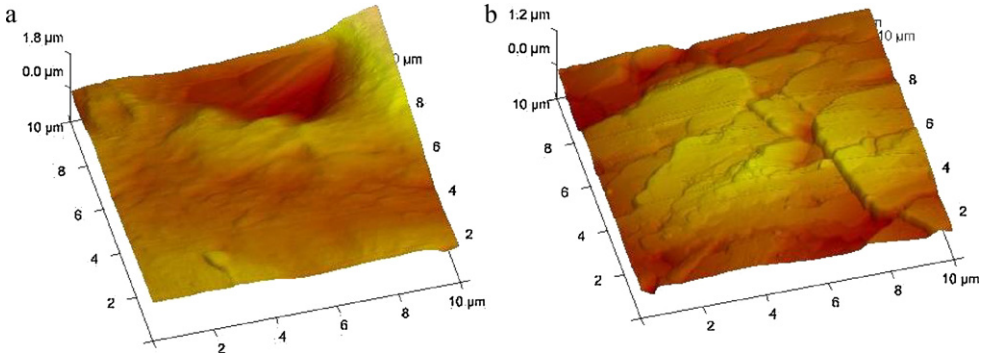

Fig. 5. AFM images of copolymer film (a) and copolymer composite film (b).

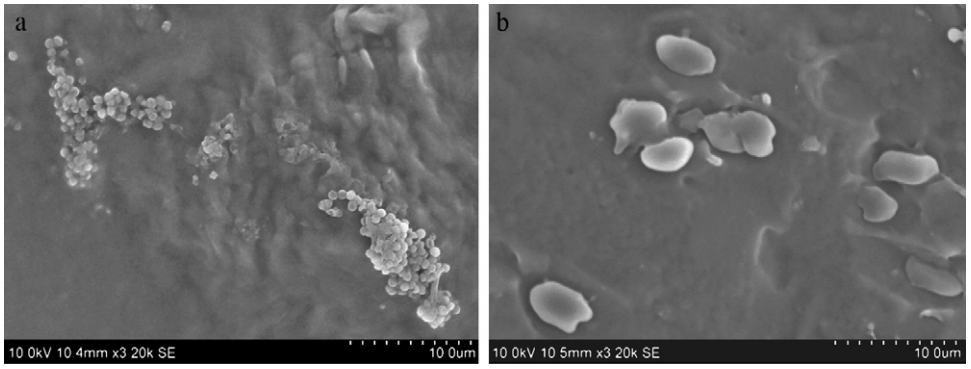

Fig. 6. SEM micrographs of *S. aureus* biofilm on (a) copolymer film and (b) copolymer composite film.

respectively. This shows that the copolymer composite film is slightly hydrophobic when compared to the copolymer film.

The composite film had lower surface energy (41.4 ± 2.8 mJ/m^2) when compared to the polymer film (47.2 ± 1.4 mJ/m^2), once again indicating that the former is more hydrophobic than the later. Surface roughness, topography, surface composition, surface free energy and hydrophilicity play an important role in implants in determining the initial protein and cell adhesion (Rupp et al., 2006).

3.4. Bacterial adhesion

Adhesion of *E. coli* and *S. aureus* onto the polymer film and copolymer composite film were evaluated quantitatively in terms of CFU (colony forming units of the viable cells) Copolymer composite polymer film showed 99.5% and 98% reduction in the adhesion of *S. aureus* and *E. coli* respect when compared to the copolymer film. Fig. 6 shows the SEM of adhered *S. aureus* on copolymer and copolymer composite films.

Copolymer composite film has lower surface roughness, and slightly higher contact angle and slightly lower surface energy when compared to the copolymer film. Decreased surface roughness leads to a decrease in bacterial adhesion (Sivakumar, Iyer, et al., 2010). Shao and Zhao (2010) also found that decrease in surface energy after silver coating leads to decrease in bacterial adhesion against one of the medical device infection associated microbe, *P. aeruginosa* PA01.

Apart from dead and live cells, bacterial biofilm comprises of proteins and exopolysaccharide which are useful in the adhesion of the bacteria on implant surfaces. Pathogenesis of infection is dependent on bacterial adhesion and protein absorption on to the biomaterial surfaces (Pavithra & Doble, 2008). Hydrophobic surfaces enhance the protein adhesion to the surfaces which in turn produce conditional layer promoting the formation of biofilm (Wang, Robertson, Spillman, & Claus, 2004). Thus hydrophilic surfaces are preferred since they reduce the bacterial adhesion

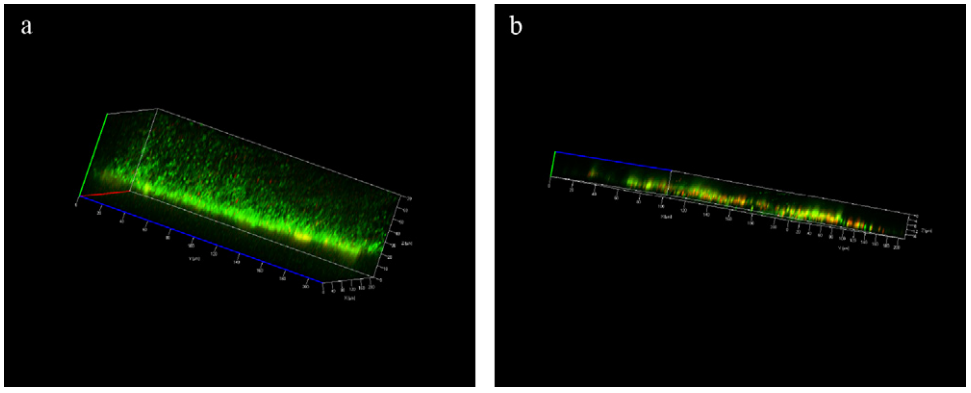

Fig. 7. Biofilm on (a) copolymer film and (b) copolymer composite film established by CLSM study.

(Bendinger, Rijnaarts, Altendorf, & Zehnder, 1993; Fletcher & Loeb, 1979; Pringle & Fletcher, 1983).

Although the copolymer composite film is slightly more hydrophobic than the copolymer film, chalcone has bactericidal (chalcones acts by cell membrane disruption which leads to bacterial cell lysis) and slimicidal activities which is the reason for the reduction in the bacterial adhesion. Previous research communications have established the cell membrane disrupting activity of chalcones (Sivakumar, Iyer, et al., 2010; Sivakumar, Kumar, et al., 2009; Sivakumar et al., 2007). Moreover, bacterial adhesion not only depends on hydrophobicity of the polymeric surface, but it also depends on the hydrophobicity of the organism surface, presence of functional group on the polymer, surface roughness, charge and flexibility, etc. Surface roughness of the copolymer composite film is lower than that of the copolymer film which also further reduces the bacterial adhesion on to the copolymer composite film.

Attached *S. aureus* cells were found on the copolymer film but they were absent in the case of copolymer composite film surface. This finding also proves that apart from bactericidal activity chalcone also has slimicidal activity. Irregular shapes observed on the copolymer composite film are not known.

3.4.1. Assessment of cell viability and mechanism of action of chalcone

In the present study, CLSM was used to analyze the biofilm and identify the distribution of live and dead cells. Chalcones are believed to act by the disruption of cell membrane. Live/Dead® BacLight™ Bacterial Viability Kit shows live cells fluoresce as green color and the dead (cell membrane damaged) cells as red color. In comparison to the biofilm on copolymer film, biofilm on copolymer composite film has more amounts of red dead cells which is due to the bactericidal action of chalcone (Fig. 7). This was also revealed in previous studies (Sivakumar, Prabhawathi, & Doble, 2010).

4. Conclusion

PCL–PEG multiblock copolymer and dimethylamino-chalcone were synthesized and characterized by FT-IR, ^{1}H NMR, ^{13}C NMR and SEC analysis. Copolymer film and copolymer composite film with dimethylamino-chalcone derivative were also prepared using the synthesized copolymer. Copolymer composite film resulted to have a lower roughness and a higher contact angle values when compared to the copolymer film. Copolymer composite film showed more than 95% reduction of adhesion of *S. aureus* and *E. coli* when compared to copolymer film. Though the copolymer composite film was found to be slightly hydrophobic than copolymer film, the reduction in bacterial adhesion was achieved due to the incorporation of the chalcone (which exerts bactericidal and slimicidal effects). CLSM and SEM studies indicated the membrane damaging effect of chalcone. Previous researchers also established the biodegradability and biocompatibility of PCL–PEG based multiblock copolymers (Cometa, Bartolozzi, et al., 2010). Hence this copolymer composite film could be proposed as biomaterial for catheter and urethral stents.

Appendix A. Supplementary data

Supplementary data associated with this article can be found, in the online version, at doi:10.1016/j.carbpol.2011.07.061.

References

Bendinger, B., Rijnaarts, H. H., Altendorf, K., & Zehnder, A. J. B. (1993). Physicochemical cell surface and adhesive properties of coryneform bacteria related to the presence and chain length of mycolic acids. *Applied Environmental Microbiology*, *59*, 3973–3977.

Boulos, L., Prévost, M., Barbeau, B., Coallier, J., & Desjardins, R. (1999). LIVE/DEAD® *Bac*Light™: Application of a new rapid staining method for direct enumeration of viable and total bacteria in drinking water. *Journal Microbiological Methods*, *37*, 77–86.

Cometa, S., Bartolozzi, I., Corti, A., Chiellini, F., De Giglio, E., & Chiellini, E. (2010). Hydrolytic and microbial degradation of multi-block polyurethanes based on poly(3-caprolactone)/poly(ethylene glycol) segments. *Polymer Degradation and Stability*, *95*, 2013–2021.

Cometa, S., Chiellini, F., Bartolozzi, I., Chiellini, E., Giglio, E. D., & Sabbatini, L. (2010). Surface segregation assessment in poly(ε-caprolactone)-poly(ethylene glycol) multiblock copolymer films. *Macromolecular Bioscience*, *10*, 317–327.

Flemming, R. G., Capelli, C. C., Cooper, S. L., & Proctor, R. A. (2000). Bacterial colonization of functionalized polyurethanes. *Biomaterials*, *21*, 273–281.

Fletcher, M., & Loeb, G. I. (1979). Influence of substratum characteristics on the attachment of a marine pseudomonad to solid surfaces. *Applied Environmental Microbiology*, *37*, 67–72.

Francolini, I., D'Ilario, L., Guaglianone, E., Donelli, G., Martinelli, A., & Piozzi, A. (2010). Polyurethane anionomers containing metal ions with antimicrobial properties: Thermal, mechanical and biological characterization. *Acta Biomaterialia*, *6*, 3482–3490.

Grapski, J. A., & Cooper, S. L. (2001). Synthesis and characterization of non-leaching biocidal polyurethanes. *Biomaterials*, *22*, 2239–2246.

Khandwekar, A. P., Patil, D. P., Shouche, Y. S., & Doble, M. (2009). Controlling biological interactions with surface entrapment-modified polyurethane. *Journal of Medical Biological Engineering*, *29*, 84–91.

Klevens, R. M., Edwards, J. R., Richards, C. L., Horan, T. C., Gaynes, R. P., Pollock, D. A., et al. (2002). Estimating health care-associated infections and deaths in US hospitals. *Public Health Reports*, *122*, 160–1666.

Lin, J., Rivett, D. E., & Wilshire, J. F. K. (1977). The preparation and photochemical properties of some 1,3-diphenyl-2-pyrazolines containing a heteroaromatic substituent. *Australian Journal Chemistry*, *30*, 629.

Liu, C. B., Gong, C. Y., Huang, M. J., Wang, J. W., Pan, Y. F., Zhang, Y. D., et al. (2008). Thermoreversible gel–sol behavior of biodegradable PCL–PEG–PCL triblock copolymer in aqueous solutions. *Journal of Biomedical Material Research Part B*, *84*, 165–175.

Liu, Y., Wu, N., Wei, Q., Cai, Y., & Wei, A. (2008). Wetting behavior of electrospun poly(L-lactic acid)/poly(vinyl alcohol) composite nonwovens. *Journal of Applied Polymer Science*, *110*, 3172–3177.

Nablo, B. J., Prichard, H. L., Butler, R. D., Klitzman, B., & Schoenfisch, M. H. (2005). Inhibition of implant-associated infections via nitric oxide release. *Biomaterials*, *26*, 6984–6990.

Nava-Ortiz, C. A. B., Burillo, G., Concheiro, A., Bucio, E., Matthijs, N., Nelis, H., et al. (2010). Cyclodextrin-functionalized biomaterials loaded with miconazole prevent *Candida albicans* biofilm formation *in vitro*. *Acta Biomaterialia*, *6*, 1398–1404.

Nielsen, S. F., Larsen, M., Boesen, T., Schønning, K., & Kromann, H. (2005). Cationic chalcone antibiotics. Design, synthesis, and mechanism of action. *Journal of Medicinal Chemistry*, *48*, 2667–2677.

Pavithra, D., & Doble, M. (2008). Biofilm formation, bacterial adhesion and host response on polymeric implants—issues and prevention. *Biomedical Materials*, *3*, 034003.

Pierce, G. E. (2005). *Pseudomonas aeruginosa*, *Candida albicans*, and device-related nosocomial infections: Implications, trends, and potential approaches for control. *Journal of Industrial Microbiology and Biotechnology*, *32*, 309–318.

Pringle, J. H, & Fletcher, M. (1983). Influence of substratum wettability on attachment of freshwater bacteria to solid surfaces. *Applied Environmental Microbiology*, *45*, 811–817.

Rupp, M. E., & Archer, G. L. (1994). Coagulase-negative staphylococci: Pathogens associated with medical progress. *Clinical Infectious Disease*, *19*, 231–245.

Rupp, F., Scheideler, L., Olshanska, N., de Wild, M., Wieland, M., & Geis-Gerstorfer, J. (2006). Enhancing surface free energy and hydrophilicity through chemical modification of microstructured titanium implant surfaces. *Journal of Biomedical Material Research Part A*, *76A*, 323–334.

Schulin, T., & Voss, A. (2001). Coagulase-negative staphylococci as a cause of infections related to intravascular prosthetic devices: Limitations of present therapy. *Clinical Infectious Disease*, *7*(Suppl. 4), 1–7.

Selvakumar, N., Kumar, G. S., Azhagan, A. M., Rajulu, C. G., Sharma, S., Kumar, M. S., et al. (2007). Synthesis SAR and antibacterial studies on novel chalcone oxazolidinone hybrids. *European Journal Medicinal Chemistry*, *42*, 538–543.

Shao, W., & Zhao, Q. (2010). Influence of reducers on nanostructure and surface energy of silver coatings and bacterial adhesion. *Surface Coatings Technology*, *204*, 1288–1294.

Sivakumar, P. M., Iyer, G., Natesan, L., & Doble, M. (2010). Applied Surface Science. *3′-Hydroxy-4-methoxychalcone as a potential antibacterial coating on polymeric biomaterials*, *256*, 6018–6024.

Sivakumar, P. M., Kumar, T. M., & Doble, M. (2009). Antifungal activity, mechanism and QSAR studies on chalcones. *Chemical Biology Drug Design*, *74*, 68–79.

Sivakumar, P. M., Prabhawathi, V., & Doble, M. (2010). 2-Methoxy-2′,4′-dichloro chalcone as an antimicrofoulant against marine bacterial biofilm. *Colloids and Surfaces: BioInterfaces B*, *81*, 439–446.

Sivakumar, P. M., Priya, S., & Doble, M. (2009). Synthesis, biological evaluation, mechanism of action and quantitative structure–activity relationship studies of chalcones as antibacterial agents. *Chemical Biology Drug Design*, *73*, 403–415.

Sivakumar, P. M., Seenivasan, S. P., Kumar, V., & Doble, M. (2007). Synthesis, antimycobacterial activity evaluation, and QSAR studies of chalcone derivatives. *Bioorganic Medicinal Chemistry Letters*, *17*, 1695–1700.

Vuong, C., & Otto, M. (2002). *Staphylococcus epidermidis* infections. *Microbes and Infection*, *4*, 481–489.

Wang, Y., Robertson, J. L., Spillman, W. B., Jr., & Claus, R. O. (2004). Effects of the chemical structure and the surface properties of polymeric biomaterials on their biocompatibility. *Pharmaceutical Research*, *21*, 1362–1373.

Zhao, Q., Liu, Y., Wang, C., Wang, S., Peng, N., & Jeynes, C. (2007). Bacterial adhesion on ion-implanted stainless steel surfaces. *Applied Surface Science*, *253*, 8674–8681.

Zhou, S., Deng, X., & Yang, H. (2003). Biodegradable poly(γ-caprolactone)-poly(ethylene glycol) block copolymers: Characterization and their use as drug carriers for a controlled delivery system. *Biomaterials*, *24*, 3563–3570.